Classical simulation of quantum entanglement using optical transverse modes in multimode waveguides

Jian Fu,[1] Zhijian Si,[1] Shaofang Tang,[2] and Jian Deng[1]

[1]*State Key Lab of Modern Optical Instrumentation, Department of Optical Engineering, Zhejiang University, Hangzhou 310027, China*

[2]*College of Science, Hangzhou Teachers' College, Hangzhou 310036, China*

(Received 13 April 2004; published 21 October 2004)

We discuss "mode-entangled states" based on the optical transverse modes of the optical field propagating in multimode waveguides, which are classical simulation of the quantum entangled states. The simulation is discussed in detail, including the violation of the Bell inequality and the correlation properties of optical pulses' group delays. The research on this simulation may be important, for it not only provides useful insights into fundamental features of quantum entanglement, but also yields interesting insights into quantum computation and quantum communication.

I. INTRODUCTION

So far, there is interest in research on classical wave analogs of the Schrodinger wave function [1–3]. It is well known that, in the paraxial approximation, the transverse modes of an optical field obey a propagation equation which is formally identical to the Schrodinger equation with the time replaced by the axial coordinate [1]. The transverse modes of the optical field propagating in a waveguide with a parabolic refractive index profile are formally identical to quantum harmonic oscillator wave functions. Some efforts have gone into researching on classical wave analogs of quantum mechanics, including analogs of Fock states and measurement of Wigner phase-space distributions for classical optical fields which can exhibit negative regions [3–6]. However, research on classical analogs has been limited principally to measurement of first-order coherence, i.e., single-particle states. Classical-wave analogs of high-order coherence (quantum entanglement), i.e., multiparticle states, have been seldom studied [7]. The quantum entanglement, which describes nonlocal quantum correlation between different degrees of freedom especially separated particles, is regarded as the inherent feature of quantum theory [8]. The quantum correlation has been shown in the correlation measurement of the entangled state, and a criterion has been given by the violation of the Bell inequality [9]. In recent research, the quantum entanglement is considered as a key property to realize the quantum computation [10] and quantum teleportation [11], which makes the quantum entanglement strongly attracted to researchers.

In this paper, we will propose "mode-entangled states" based on the optical transverse modes of the optical field propagating in multimode waveguides. It is well known that the quantum entanglement is the characteristic of the quantum theory with no classical analog. Therefore the mode-entangled states should be interpreted as the classical simulation of quantum entanglement using the optical transverse modes of the optical fields. The classical simulation will be discussed in detail, including the violation of the Bell inequality and the correlation properties of optical pulses'

group delays. In Ref. [12], a full optical scheme to perform quantum computation is proposed, based on the optical transverse modes in multimode waveguides. The proposed controlled-NOT (CNOT) gate has the potential of being easily realized since it is based on optical waveguide technology and can be constructed by using Mach-Zehnder interferometer having semiconductor optical amplifiers (SOA's) in its arms. The SOA can provide a very large Kerr-like nonlinearity even at relatively low light intensities and can avoid the intensity attenuation excited by two-photon absorption [13]. Therefore SOA's have been used extensively as nonlinear elements in optical switching and wavelength-conversion devices [14]. But whether the scheme would be capable of implementing the quantum computation depends on whether the CNOT gate proposed in Ref. [12] can generate the mode-entangled states. Given all these, the research on the similarity between the mode-entangled states and the quantum entangled states may be important, for it not only provides a useful insight into fundamental features of quantum entanglement, but also yields interesting insights into quantum computation and quantum communication.

The paper is organized as follows: In Sec. II, we will discuss the analogies between optical transverse modes in a multimode waveguide and quantum Fock states. In Sec. III, the superposition of transverse modes in a random waveguide is analyzed. In Sec. IV, the Bell inequality as a criterion of the existence of mode-entangled states is deduced. In Sec. V, an analysis of the mode-entangled states in random waveguides and the correlation properties of group delays is discussed. Finally, we summarize our conclusions in Sec. VI.

II. ANALOGS OF QUANTUM FOCK STATES USING OPTICAL TRANSVERSE MODES

Considering a weakly guiding, symmetric slab waveguide, an optical field in the propagation direction, longitudinal z direction, is restricted within the core region, which has the higher refractive index (RI) compared with that of the cladding. By using the Fock-Leontovich paraxial approximation, the Maxwell equations for the monochromatic electric

field component can be reduced to the equivalent Schrodinger equation. The reduced field [1]

$$\Psi(x,y,z) = \sqrt{n_0} E(x,y,z) \exp\left(-ik\int_0^z n_0 dz\right) \quad (1)$$

satisfies the following equation:

$$\frac{i}{k}\frac{\partial\Psi}{\partial\xi} = -\frac{1}{2k^2}(\nabla_x^2\Psi + \nabla_y^2\Psi) + \frac{1}{2}[n_0^2 + n^2(x,y,z)]\Psi = H\Psi,$$

$$(2)$$

where $E(x,y,z)$ is the monochromatic electric-field component, the geometry of the waveguide is defined by the RI profile $n(x,y,z)$, $n_0 = n(0,0,z)$, $k = 2\pi/\lambda$ (with λ being the wavelength in free space), and $\xi = \int_0^z dz/n_0$. Therefore when the RI profile $n(x,y,z)$ is parabolic, Eq. (2) is similar to the Schrodinger equation for a quantum harmonic oscillator. Here, instead of Plank's constant h, we have the vacuum light wavelength λ. And the variable ξ plays the role of time. Following Ref. [15], coordinate and momentum operators $\hat{X}_i$ and $\hat{P}_i = -(i/k)(\partial/\partial x_i)$ ($i = 1,2$ denote x and y, respectively) can be introduced. These operators obey the standard commutation relations $[\hat{X}_i, \hat{P}_j] = (i/k)\delta_{ij}$ and uncertain relations $(\Delta X_i)^2(\Delta P_i)^2 \geq (1/4k^2)$, where $(\Delta X_i)^2 = \langle\hat{X}_i^2\rangle - \langle\hat{X}_i\rangle^2$ and $(\Delta P_i)^2 = \langle\hat{P}_i^2\rangle - \langle\hat{P}_i\rangle^2$.

When the optical field propagates in the waveguide that is z invariant, in other words, the RI profile is uniform along z, the propagation can be equivalently described in the time-independent Schrodinger equation

$$H\Psi_n(x,y) = \omega_n\Psi_n(x,y), \quad (3)$$

where $\Psi_n(x,y)$ are a set of eigenmodes corresponding to a set of discrete eigenvalues ω_n. It leads to the expression of the monochromatic electric field component $E(x,y,z)$ as follows:

$$E(x,y,z) = \sum_n C_n e^{-i\beta_n z}\Psi_n(x,y), \quad (4)$$

where the propagation constants β_n are given as

$$\beta_n = k(n_0^2 - 2\omega_n)^{1/2}. \quad (5)$$

As described in Ref. [3], such eigenmodes $\Psi_n(x,y)$ are similar to the quantum Fock states. Here we introduce the annihilation operators $\hat{a}_i = \sqrt{k/2}(\hat{X}_i + i\hat{P}_i)$ and the creation operators $\hat{a}_i^+ = \sqrt{k/2}(\hat{X}_i - i\hat{P}_i)$ that obey the boson commutation relations $[\hat{a}_i^+, \hat{a}_j] = \delta_{ij}$, $[\hat{a}_i, \hat{a}_j] = [\hat{a}_i^+, \hat{a}_j^+] = 0$. Application of the creation and annihilation operators to the Fock states yield

$$\hat{a}^+|n\rangle = \sqrt{n+1}|n+1\rangle,$$

$$\hat{a}|n\rangle = \sqrt{n}|n-1\rangle, \quad (6)$$

$$\hat{a}^+\hat{a}|n\rangle = n|n\rangle,$$

where $|n\rangle$ are the eigenmodes $\Psi_n(x)$, $n = 0,1,2,\ldots$ (for simplicity only x direction is considered).

It is well known that random perturbations of the geometry of multimode optical waveguides cause fluctuations of the average arrival time (group delay) and spread (dispersion) of optical pulse propagating in the waveguides [16–20]. In general, the information given for the description of optical field propagation in a random waveguide by means of the field $\Psi(x,y,z)$ in Eq. (1) is not complete. The optical field propagation may be generally described by means of the density-matrix formalism [1]

$$\rho = \sum_{mn}\rho_{mn}|m\rangle\langle n|, \quad (7)$$

which satisfies the Liouville equation

$$i\frac{\partial\rho}{\partial z} = [H,\rho]. \quad (8)$$

The density matrix possesses the usual properties: $\text{Tr}\,\rho = 1$, $\text{Tr}\,\rho^2 \leq 1$ (the equality is true for pure states). The expectation value of any operator $\hat{Q}$ is given by the trace of the product of ρ and $\hat{Q}$: $\langle Q\rangle = \text{Tr}(\rho\hat{Q})$. Therefore the utilization of the density-matrix formalism seems to be useful for describing a superposition of modes in the random waveguide.

III. SUPERPOSITION OF TRANSVERSE MODES IN A RANDOM WAVEGUIDE

In Ref. [12], a full optical method based on the transverse eigenmodes is proposed to perform the quantum computation, in which TE_0 mode and TE_1 mode in dual-mode waveguide are used as qubits to represent logical 0 and 1. In this section, we will use the density-matrix formalism in the analysis of superposition of these two modes (TE_0 mode and TE_1 mode) in a random waveguide.

The superposition of the modes can be described as

$$\Psi(x,y,z) = C_0 e^{-i\beta_0 z}|TE_0\rangle + C_1 e^{-i\beta_1 z}|TE_1\rangle, \quad (9)$$

where β_0 and β_1 are the propagation constants of the modes $|TE_0\rangle$ and $|TE_1\rangle$, respectively. In the dual-mode waveguide, the coupling of TE0 mode and TE1 mode is similar to a two-level system. Thus to describe this kind of coupling, we introduce the Hamiltonian

$$H = \beta_0\left(\hat{a}^\dagger\hat{a} + \frac{1}{2}\right) + \beta_1\left(\hat{b}^\dagger\hat{b} + \frac{1}{2}\right) + C_{ab}\hat{a}^\dagger\hat{b} + C_{ab}^*\hat{b}^\dagger\hat{a},$$

$$(10)$$

where $\hat{a}^+$ and $\hat{a}$ are the creation and the annihilation operators of the mode $|TE_0\rangle$, and $\hat{b}^+$ and $\hat{b}$ are the creation and the annihilation operators of the mode $|TE_1\rangle$. In the random waveguide, the random coupling among the guided modes will be caused by the perturbations in the waveguide geometry. Here we introduce a coupling coefficient to describe the random coupling. The coupling coefficients are functions of z coordinate that measures distance along the waveguide axis. In random waveguides, the coupling coefficient assume the form [21]

$$C_{ab} = K_{ab}f(z), \tag{11}$$

where K_{ab} is independent of z. The function $f(z)$ often describes the actual shape of the deformed waveguide boundary or the bent waveguide axis. And it is supposed to be a stationary random variable whose correlation function is assumed to be Gaussian

$$\langle f(z)f(z-u)\rangle = \sigma^2 e^{-(u/D)^2} \tag{12}$$

where $\langle \cdots \rangle$ denotes the average over an ensemble of random realizations, σ is the variance, and D is the correlation length of $f(z)$.

To study effects on the superposition of transverse eigenmodes caused by this kind of randomicity, we introduce the density matrix ρ. If we rewrite the modes $|\text{TE}_0\rangle$ and $|\text{TE}_1\rangle$ as

$$|\text{TE}_0\rangle = \begin{pmatrix} 1 \\ 0 \end{pmatrix}, \quad |\text{TE}_1\rangle = \begin{pmatrix} 0 \\ 1 \end{pmatrix}, \tag{13}$$

the density matrix ρ of the mode superposition (9) can also be rewritten,

$$\rho = \begin{pmatrix} |C_0|^2 & C_0 C_1^* e^{i\Delta\beta z} \\ C_1 C_0^* e^{-i\Delta\beta z} & |C_1|^2 \end{pmatrix}, \tag{14}$$

where $\Delta\beta = \beta_1 - \beta_0$. The Liouville equation (8) can be written in the equivalent form

$$i\frac{\partial \rho_{mn}(z)}{\partial z} = (\beta_m - \beta_n)\rho_{mn}(z) + \langle [V(z), \rho(z)]\rangle_{mn}, \tag{15}$$

where $m, n \in \{0,1\}$, $V(z) = C_{ab}\hat{a}^+\hat{b} + C_{ab}^*\hat{b}^+\hat{a}$. By using the method mentioned in Ref. [18], after the optical field propagates a distance of L in the random waveguide, the density matrix ρ can be described as

$$\rho = \begin{pmatrix} (1+e^{-2\gamma L})\dfrac{|C_0|^2}{2} + (1-e^{-2\gamma L})\dfrac{|C_1|^2}{2} & C_0 C_1^* e^{[i(\Delta\beta+\kappa)-\gamma]L} \\ C_1 C_0^* e^{[-i(\Delta\beta+\kappa)-\gamma]L} & (1+e^{-2\gamma L})\dfrac{|C_1|^2}{2} + (1-e^{-2\gamma L})\dfrac{|C_0|^2}{2} \end{pmatrix}, \tag{16}$$

where

$$\gamma = \sqrt{\pi}\sigma^2 D e^{-(D\Delta\beta/2)^2}|K_{ab}|^2, \tag{17}$$

$$\kappa = \text{Im}[\sqrt{\pi}\sigma^2 D e^{-(D\Delta\beta/2)^2}\,\text{erf}(iD\Delta\beta/2)|K_{ab}|^2].$$

We have assumed so far that $\Delta\beta \gg \gamma$, $\Delta\beta \gg \kappa$ and the waveguide is lossless. From Eq. (16), we can anticipate if $L \to \infty$, $\text{Tr}\,\rho^2 \to \frac{1}{2}$, which shows the evolution from the coherence (pure state) superposition to the incoherence (mixed state) superposition caused by the perturbation in the random waveguide.

In order to distinguish between the coherence superposition and the incoherence superposition, we propose a scheme by analyzing the symmetries of the eigenmodes. In Fig. 1, the profiles of the modes $|\text{TE}_0\rangle$ and $|\text{TE}_1\rangle$ are shown, $|\text{TE}_0\rangle$ is symmetric and $|\text{TE}_1\rangle$ is antisymmetric. A Y splitter is a device to split one light beam into two beams. If the perturbation of the Y splitter's transition is slight (i.e., the change of propagation constant $\Delta\beta \approx 0$), the splitter can split the beam with extremely low power loss. When $|\text{TE}_0\rangle$ and $|\text{TE}_1\rangle$ are launched in the Y splitter, $|\text{TE}_0\rangle$ is split into two symmetric parts, while $|\text{TE}_1\rangle$ is split into two antisymmetric parts [22]. Therefore the output states of the Y splitter's two branches are given explicitly by

$$|+\rangle = \frac{1}{\sqrt{2}}(|\text{TE}_0\rangle + |\text{TE}_1\rangle), \tag{18}$$

$$|-\rangle = \frac{1}{\sqrt{2}}(|\text{TE}_0\rangle - |\text{TE}_1\rangle).$$

When the input of Y splitter is given at a coherence superposition, $|\Psi_{in}\rangle = (1/\sqrt{2})(e^{-i\theta}|\text{TE}_0\rangle + e^{i\theta}|\text{TE}_1\rangle)$, via expanding the input states in terms of the output states of the two branches of the splitter, we got $|\Psi_{in}\rangle = \cos\theta|+\rangle - i\sin\theta|-\rangle$, from which the intensities of two branches can be obtained,

$$|\langle +|\Psi_{in}\rangle|^2 = \cos^2\theta, \tag{19}$$
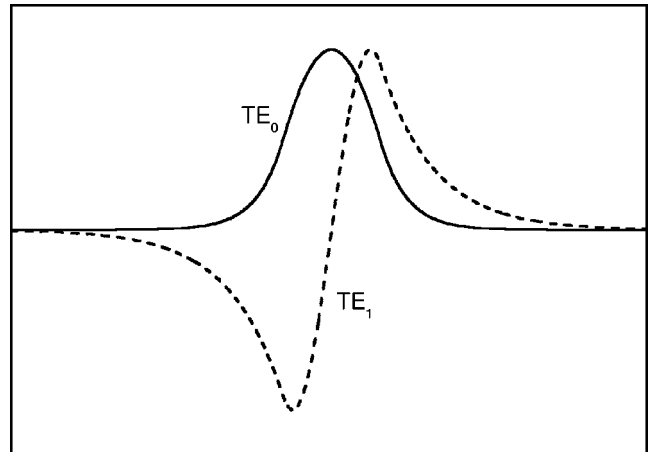

FIG. 1. Electric-field profiles for the optical transverse modes TE$_0$ (the symmetric mode) and TE$_1$ (the antisymmetric mode).

$$|\langle -|\Psi_{in}\rangle|^2 = \sin^2\theta.$$

Note that the phase θ of the input field $|\Psi_{in}\rangle$ will cause the variation of intensity in the Y splitter's two branches. When the input of the Y splitter is given at an incoherence superposition, the relationship of the phase between the modes $|TE_0\rangle$ and $|TE_1\rangle$ is uncertain. The density matrix of the incoherence superposition is given as

$$\rho = \sum_{n=0,1} W_n |TE_n\rangle\langle TE_n|, \tag{20}$$

where $W_n = \frac{1}{2}$ are the probabilities for the two modes $|TE_0\rangle$ and $|TE_1\rangle$. Then the output average intensities in two branches are $\langle +|\rho|+\rangle = \langle -|\rho|-\rangle = \frac{1}{2}$. It shows that when the input is at the incoherence superposition, no matter how the phase of the input changes, the output intensities will stay invariable. That is the essence of our scheme of measuring the intensity difference between the Y splitter's two branches to distinguish between the coherence superposition and the incoherence superposition.

Now, we apply the Y splitter to the analysis of the superposition state that is the evolution of a coherence superposition state after propagating in a random waveguide with distance of L. We define operators to represent the operations of a phase controller and Y splitter,

$$\hat{I}^+(\theta) = \hat{P}^+(\theta)|+\rangle\langle +|\hat{P}(\theta) = \frac{1}{2}\begin{pmatrix} 1 & e^{2i\theta} \\ e^{-2i\theta} & 1 \end{pmatrix}, \tag{21}$$

$$\hat{I}^-(\theta) = \hat{P}^+(\theta)|-\rangle\langle -|\hat{P}(\theta) = \frac{1}{2}\begin{pmatrix} 1 & -e^{2i\theta} \\ -e^{-2i\theta} & 1 \end{pmatrix},$$

where $\hat{P}(\theta)$ denotes the phase control of the input state

$$\hat{P}(\theta)|\Psi\rangle = \hat{P}(\theta)(C_0|TE_0\rangle + C_1|TE_1\rangle)$$
$$= C_0 e^{-i\theta}|TE_0\rangle + C_1 e^{i\theta}|TE_1\rangle. \tag{22}$$

The control of the phase difference between the two modes $|TE_0\rangle$ and $|TE_1\rangle$ can be achieved by properly changing the RI of the core layer [22].

After the input at a mode superposition state propagates a distance of L in the random waveguide and passes through a phase controller and a Y splitter, the intensity difference between the output waveguides can be obtained by using the density matrix ρ in Eq. (16),

$$\langle \hat{I}^+(\theta) - \hat{I}^-(\theta)\rangle = \text{Tr}\{\rho[\hat{I}^+(\theta) - \hat{I}^-(\theta)]\}$$
$$= e^{-\gamma L}[C_0 C_1^* e^{i(\Delta\beta+\kappa)L} e^{2i\theta}$$
$$+ C_1 C_0^* e^{-i(\Delta\beta+\kappa)L} e^{-2i\theta}]. \tag{23}$$

When $C_0 = C_1 = 1/\sqrt{2}$, $\langle \hat{I}^+(\theta) - \hat{I}^-(\theta)\rangle = e^{-\gamma L}\cos[2\theta + (\Delta\beta + \kappa)L]$. It is already obvious that the perturbation in the waveguide geometry may cause the evolution from the coherence superposition to the incoherence superposition, namely decoherence, which leads to disappearance of the intensity difference between two outputs of the Y splitter.

By using beam propagation method (BPM) [23], we calculate numerically the behavior of the mode superposition in
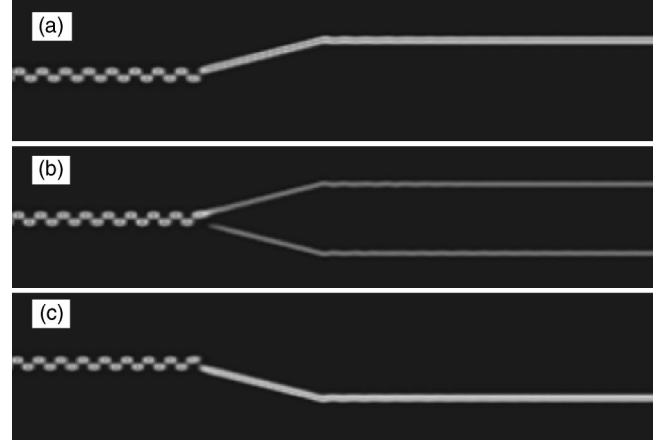

FIG. 2. The intensity variances of the Y splitter's two branches by changing the RI of the core layer (the length $L=1$ mm): (a) $\Delta n = 0$, (b) $\Delta n = 0.0001$, (c) $\Delta n = 0.000\,21$.

the dual waveguide when it is propagating in the phase controller and the Y splitter discussed above. The results are shown in Fig. 2, which show that the intensities of Y splitter's two branches vary by changing the RI of the core layer.

IV. BELL INEQUALITY OF OPTICAL TRANSVERSE MODE ENTANGLEMENT

As shown in Ref. [3], in the Wigner distribution, the optical transverse modes are similar to quantum Fock states. However, such similarities are confined to first-order coherence (such as single particle). The higher-order coherence (such as multiparticle) is regarded as the inherent feature of quantum phenomena, which is nonlocal quantum correlation shown in the correlation measurement of the quantum entangled state. The criterion of the existence of the quantum entanglement is given by the violation of the Bell inequality. In this section, we will discuss the correlation properties of the optical mode entanglement that is classical simulation of the quantum entanglement.

We assume that a kind of mode-entangled states can be generated by means of some kind of interaction between the optical fields propagating in multimode waveguides (e.g., the CNOT gate proposed in Ref. [12]). The mode-entangled states are given as

$$|\Phi_1^\pm\rangle = \frac{1}{\sqrt{2}}(|TE_0\rangle_c|TE_0\rangle_t \pm |TE_1\rangle_c|TE_1\rangle_t), \tag{24}$$

$$|\Psi_1^\pm\rangle = \frac{1}{\sqrt{2}}(|TE_0\rangle_c|TE_1\rangle_t \pm |TE_1\rangle_c|TE_0\rangle_t),$$

where c and t represent the control and the target fields, respectively. The states in each waveguide are a mode superposition, but they are different from a product state,

$$|\Psi_2\rangle = \frac{1}{2}(|TE_0\rangle_c + |TE_1\rangle_c)(|TE_0\rangle_t + |TE_1\rangle_t). \tag{25}$$

The difference of $|\Phi_1^\pm\rangle$ ($|\Psi_1^\pm\rangle$) and $|\Psi_2\rangle$ can be obtained not by measuring a single field, but by the correlation measure-
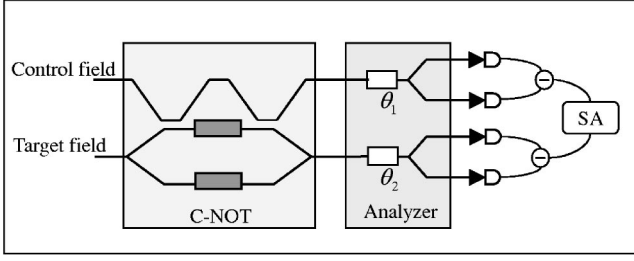
FIG. 3. Experimental scheme. The input of control field is given at the mode superposition $1/\sqrt{2}\,(|TE_0\rangle + |TE_1\rangle)$ and the input of target field is given at the mode $|TE_0\rangle$ or $|TE_1\rangle$. Then the output fields of the CNOT gate are sent to spatially separated mode analyzers, each of which contains a Y splitter and a variable phase control θ_1 (θ_2). The detected photocurrents are passively subtracted and monitored on a spectrum analyzer (SA) to check for correlations.

ment of the control and the target fields. This correlation measurement can show that the two entangled fields are impartible to some extent. Similar to quantum entanglement, the violation of the Bell inequality is also used as the criterion of this impartibility.

To perform the correlation measurement of the Bell inequality, a mode analyzer with a phase controller is required. The construction mentioned in the last section consisting of a phase controller and a Y splitter meets the requirements. Following Eq. (21), we define operators $\hat{I}_1^{\pm}$ and $\hat{I}_2^{\pm}$ to represent the mode analyzer's operations on the control and the target fields, respectively,

$$\hat{I}_1^+ - \hat{I}_1^- = \hat{P}^+(\theta_1)(|+\rangle_c\langle+|_c - |-\rangle_c\langle-|_c)\hat{P}(\theta_1)$$
$$= e^{2i\theta_1}|TE_1\rangle_c\langle TE_0|_c + e^{-2i\theta_1}|TE_0\rangle_c\langle TE_1|_c, \quad (26)$$

$$\hat{I}_2^+ - \hat{I}_2^- = \hat{P}^+(\theta_2)(|+\rangle_t\langle+|_t - |-\rangle_t\langle-|_t)\hat{P}(\theta_2)$$
$$= e^{2i\theta_2}|TE_1\rangle_t\langle TE_0|_t + e^{-2i\theta_2}|TE_0\rangle_t\langle TE_1|_t,$$

where $\hat{P}(\theta_1)$ and $\hat{P}(\theta_2)$ represent the phase controllers on the control and the target fields, respectively. As discussed in Sec. III, when θ_1 and θ_2 change, the output intensities of the Y splitters will vary correspondingly.

Based on the correlation analysis, we propose an experimental scheme, shown in Fig. 3, in which the mode-entangled state is generated via the CNOT gate proposed in Ref. [12]. The input of control field is given at the mode superposition $1/\sqrt{2}\,(|TE_0\rangle + |TE_1\rangle)$ and the input of target field is given at the mode $|TE_0\rangle$ or $|TE_1\rangle$. Then the output fields of the CNOT gate are sent to spatially separated mode analyzers represented by $\hat{I}_1^{\pm}$ and $\hat{I}_2^{\pm}$. The detected photocurrents of the mode analyzers' outputs are passively subtracted and monitored on a spectrum analyzer (SA) to check for correlations. Therefore the correlation function is given by

$$E(\theta_1, \theta_2) = \frac{\langle(\hat{I}_1^+ - \hat{I}_1^-)(\hat{I}_2^+ - \hat{I}_2^-)\rangle}{\langle(\hat{I}_1^+ + \hat{I}_1^-)(\hat{I}_2^+ + \hat{I}_2^-)\rangle}. \quad (27)$$

Substituting $|\Phi_1^+\rangle$ and $|\Psi_2\rangle$ into Eq. (27), respectively, we obtain the correlation functions of the two states,
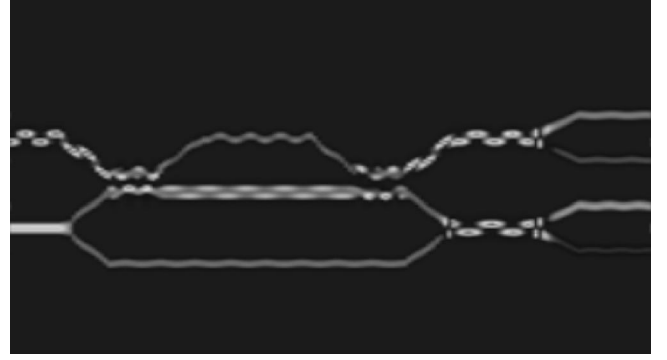

FIG. 4. BPM simulation result for the scheme shown in Fig. 3.

$$E_{\Phi_1^+}(\theta_1, \theta_2) = \frac{\langle(\hat{I}_1^+ - \hat{I}_1^-)(\hat{I}_2^+ - \hat{I}_2^-)\rangle}{\langle(\hat{I}_1^+ + \hat{I}_1^-)(\hat{I}_2^+ + \hat{I}_2^-)\rangle} = \frac{\langle\Phi_1^+|(\hat{I}_1^+ - \hat{I}_1^-)(\hat{I}_2^+ - \hat{I}_2^-)|\Phi_1^+\rangle}{\langle\Phi_1^+|(\hat{I}_1^+ + \hat{I}_1^-)(\hat{I}_2^+ + \hat{I}_2^-)|\Phi_1^+\rangle}$$
$$= \cos(2\theta_1 + 2\theta_2), \quad (28)$$

$$E_{\Psi_2}(\theta_1, \theta_2) = \frac{\langle(\hat{I}_1^+ - \hat{I}_1^-)(\hat{I}_2^+ - \hat{I}_2^-)\rangle}{\langle(\hat{I}_1^+ + \hat{I}_1^-)(\hat{I}_2^+ + \hat{I}_2^-)\rangle} = \frac{\langle\Psi_2|(\hat{I}_1^+ - \hat{I}_1^-)(\hat{I}_2^+ - \hat{I}_2^-)|\Psi_2\rangle}{\langle\Psi_2|(\hat{I}_1^+ + \hat{I}_1^-)(\hat{I}_2^+ + \hat{I}_2^-)|\Psi_2\rangle}$$
$$= \cos(2\theta_1)\cos(2\theta_2). \quad (29)$$

Then we substitute the correlation functions above into the Bell inequality,

$$|B| = |E(\theta_1, \theta_2) - E(\theta_1, \theta_2') + E(\theta_1', \theta_2') + E(\theta_1', \theta_2)| \leq 2. \quad (30)$$

This particular Bell inequality is known as Clause-Horne-Shimony-Holt (CHSH) inequality [9]. For the entangled state $|\Phi_1^+\rangle$, when we choose $\theta_1 = \pi/8$, $\theta_1' = -\pi/8$, $\theta_2 = 0$, $\theta_2' = \pi/4$, we get $|B| = 2\sqrt{2}$. Obviously, by proper choice of the phases θ_1 and θ_2 in Eq. (26), the correlation of the analyzers can exhibit a maximum violation of the Bell inequality $|B| > 2$. However, the violation never occurs for the product state $|\Psi_2\rangle$.

We have simulated numerically the scheme shown in Fig. 3 by using BPM. The result is illustrated in Fig. 4. Due to the limitation of the simulation, we cannot get the correlation of the control and the target fields. Therefore the experiment is necessary to validate whether there are mode-entangled states similar to quantum entangled states.

V. OPTICAL MODE-ENTANGLED STATES IN RANDOM WAVEGUIDES

As shown in Sec. IV, the Bell inequality will be violated in the correlation measurement of a mode-entangled state. However, we can see from Eq. (23) that the violation will vanish due to perturbations of the random waveguides. The perturbations cause fluctuations of the average arrival time

(group delay) and spread (dispersion) of optical pulse propagating in the random waveguides. In this section, we will further discuss the difference of the entangled states $|\Phi_1^{\pm}\rangle$ ($|\Psi_1^{\pm}\rangle$) and the product state $|\Psi_2\rangle$ by analyzing the correlation properties of the group delays. And this difference is another proof of the existence of the mode-entangled states mentioned in the last section.

After the control and the target fields of the mode-entangled state $|\Phi_1^+\rangle$ propagate respectively in two random waveguides with the same random characteristic (the variance σ and the correlation length D) and the same distance of L, the density matrix ρ can be described as

$$\rho_{\Phi_1^+} = \frac{1}{2}\begin{pmatrix} 1 & 0 & 0 & e^{2[i(\Delta\beta+\kappa)-\gamma]L} \\ 0 & 0 & 0 & 0 \\ 0 & 0 & 0 & 0 \\ e^{2[-i(\Delta\beta+\kappa)-\gamma]L} & 0 & 0 & 1 \end{pmatrix}. \quad (31)$$

Due to the perturbations of the random waveguides, the coherent properties of mode superposition of the control and the target fields will decay exponentially with increasing the distance of L, until the whole state evolves to an incoherent superposition of $|TE_0\rangle_c|TE_0\rangle_t$ and $|TE_1\rangle_c|TE_1\rangle_t$. Similarly, the density matrix ρ of the product state $|\Psi_2\rangle$ propagating in the random waveguides can be described as

$$\rho_{\Psi_2} = \frac{1}{4}\begin{pmatrix} 1 & e^{[i(\Delta\beta+\kappa)-\gamma]L} & e^{[i(\Delta\beta+\kappa)-\gamma]L} & e^{2[i(\Delta\beta+\kappa)-\gamma]L} \\ e^{[-i(\Delta\beta+\kappa)-\gamma]L} & 1 & e^{-2\gamma L} & e^{[i(\Delta\beta+\kappa)-\gamma]L} \\ e^{[-i(\Delta\beta+\kappa)-\gamma]L} & e^{-2\gamma L} & 1 & e^{[i(\Delta\beta+\kappa)-\gamma]L} \\ e^{2[-i(\Delta\beta+\kappa)-\gamma]L} & e^{[-i(\Delta\beta+\kappa)-\gamma]L} & e^{[-i(\Delta\beta+\kappa)-\gamma]L} & 1 \end{pmatrix}. \quad (32)$$

When $L \rightarrow \infty$, the state $|\Psi_2\rangle$ evolves to an incoherent superposition of $|TE_0\rangle_c|TE_0\rangle_t$, $|TE_1\rangle_c|TE_1\rangle_t$, $|TE_1\rangle_c|TE_0\rangle_t$, and $|TE_0\rangle_c|TE_1\rangle_t$, which is obviously different from the evolution of the mode-entangled state $|\Phi_1^+\rangle$. And the difference can be shown by a correlation measurement of group delays.

The group delay of an optical pulse in a waveguide can be expressed as

$$\tau = \frac{L}{c}\frac{d\beta}{dk}, \quad (33)$$

where β is the propagation constant, c is the light velocity, and L is the length of waveguide. If we introduce the group delay operator $\hat{\tau}$ whose eigenvalues are the group delay τ, the average arrival time of the optical pulse can be obtained as follows:

$$\langle\tau(L)\rangle = \text{Tr}(\rho\hat{\tau}). \quad (34)$$

To study the correlation measurement of the group delays, we define the correlation function between the group delays of the control and the target fields as

$$\langle\tau_c, \tau_t\rangle = \langle(\hat{\tau}_c - \langle\hat{\tau}_c\rangle)(\hat{\tau}_t - \langle\hat{\tau}_t\rangle)\rangle = \langle\hat{\tau}_c\hat{\tau}_t\rangle - \langle\hat{\tau}_c\rangle\langle\hat{\tau}_t\rangle. \quad (35)$$

Substituting Eqs. (31) and (32) into Eq. (35), the correlation functions of the entangled state $|\Phi_1^+\rangle$ and the product state $|\Psi_2\rangle$ are obtained,

$$\langle\tau_c, \tau_t\rangle_{\Phi_1^+} = \text{Tr}(\rho_{\Phi_1^+}\hat{\tau}_c\hat{\tau}_t) - \text{Tr}(\rho_{c1}\hat{\tau}_c)\text{Tr}(\rho_{t1}\hat{\tau}_t)$$
$$= \frac{L^2}{4c^2}\left(\frac{d\beta_1}{dk} - \frac{d\beta_0}{dk}\right)^2 = \frac{1}{4}[t_1(L) - t_0(L)]^2, \quad (36)$$

$$\langle\tau_c, \tau_t\rangle_{\Psi_2} = \text{Tr}(\rho_{\Psi_2}\hat{\tau}_c\hat{\tau}_t) - \text{Tr}(\rho_{c2}\hat{\tau}_c)\text{Tr}(\rho_{t2}\hat{\tau}_t) = 0, \quad (37)$$

where the reduced density matrices ρ_{c1}, ρ_{t1}, ρ_{c2} and ρ_{t2} are the partial traces $\text{Tr}_t(\rho_{\Phi_1^+})$, $\text{Tr}_c(\rho_{\Phi_1^+})$, $\text{Tr}_t(\rho_{\Psi_2})$, and $\text{Tr}_c(\rho_{\Psi_2})$, respectively. Here $t_0(L)$ and $t_1(L)$ are the propagation time in the waveguide with distance of L for the modes $|TE_0\rangle$ and $|TE_1\rangle$, respectively. From Eqs. (36) and (37), we can see the difference of the correlation properties of the two states' group delays. Considerable attention should be paid to that the correlation of the entangled state will increase, instead of decrease, when the propagation distance of L increases. Such effects should be able to be observed by means of the experimental methods shown in [24–26].

VI. CONCLUSIONS

We have demonstrated some properties of the mode-entangled states as the classical simulation of the quantum entangled states. These properties can be regarded as the proofs of the existence of the mode-entangled states. Then two experimental schemes to demonstrate these properties are suggested. One is based on the violation of the Bell inequality, the other on the correlation properties of the optical pulses' group delay in random waveguides. As far as we know, both of the two schemes can be carried out in current experimental conditions. We are looking forward to performing relevant experimental schemes.

[1] S. G. Krivoshlykov and I. N. Sissakian, Opt. Quantum Electron. **12**, 463 (1980); S. G. Krivoshlykov, *Quantum-Theoretical Formalism for Inhomogeneous Graded-Index Waveguides* (Akademie Verlag, Berlin, 1994).

[2] G. Nienhuis and L. Allen, Phys. Rev. A **48**, 656 (1993).

[3] D. Dragoman, Prog. Opt. **42**, 424 (2002); D. Dragoman, Optik (Stuttgart) **111**, 393 (2000); D. Dragoman, Optik (Stuttgart) **111**, 179 (2000).

[4] C. Iaconis and I. A. Walmsley, Opt. Lett. **21**, 1783 (1996).

[5] C.-C. Cheng and M. G. Raymer, Phys. Rev. Lett. **82**, 4807 (1999).

[6] K. F. Lee, R. Reil, S. Bali, A. Wax, and J. E. Thomas, Opt. Lett. **24**, 1370 (1999).

[7] K. F. Lee and J. E. Thomas, Phys. Rev. Lett. **88**, 097902 (2002).

[8] M. A. Nielsen and I. L. Chuang, *Quantum Computation and Quantum Information* (Cambridge University Press, Cambridge, England, 2000), Chap. 4.

[9] J. S. Bell, Physica (Amsterdam) **1**, 195 (1964); J. F. Clauser, M. A. Horne, A. Shimony, and R. A. Holt, Phys. Rev. Lett. **49**, 1804 (1969).

[10] R. Jozsa and N. Linden, e-print quant-ph/0201143; D. A. Lidar, Appl. Phys. Lett. **80**, 2419 (2002); A. Ekert and R. Jozsa, Philos. Trans. R. Soc. London, Ser. A **356**, 1769 (1998).

[11] C. H. Bennett, G. Brassard, C. Crepeau, R. Jozsa, A. Peres, and W. K. Wootters, Phys. Rev. Lett. **70**, 1895 (1993).

[12] J. Fu, Proc. SPIE **5105**, 225 (2003); e-print quant-ph/0211038.

[13] X. Yang, D. Lenstra, G. D. Khoea, and H. J. S. Dorren, Opt. Commun. **223**, 169 (2003); H. J. S. Dorren, G. D. Khoea, and D. Lenstra, *ibid.* **205**, 247 (2002); A. E. Kelly *et al.*, Electron. Lett. **35**, 1477 (1999); K. E. Stubkjaer, IEEE J. Sel. Top. Quantum Electron. **6**, 1428 (2000); A. Kloch *et al.*, IEICE Trans. Electron. **E82-C**, 1475 (1999); I. Glesk *et al.*, Acta Phys. Slov. **51**, 151 (2001).

[14] D. Cotter *et al.*, Science **286**, 1523 (1999); T. Durhuus *et al.*, J. Lightwave Technol. **14**, 942 (1996).

[15] D. Marcuse, *Light Transmission Optics* (Van Nostrand Reinhold, New York, 1972).

[16] M. Rousseau and J. Arnaud, Opt. Quantum Electron. **10**, 53 (1978).

[17] L. Jeunhomme and J. P. Pocholle, Appl. Opt. **17**, 463 (1978).

[18] D. Marcuse, Bell Syst. Tech. J. **51**, 1199 (1972); **48**, 3187 (1969).

[19] J. A. Arnaud, Bell Syst. Tech. J. **53**, 1599 (1974); **49**, 2311 (1970).

[20] D. Gloge and E. A. J. Marcatili, Bell Syst. Tech. J. **52**, 1563 (1973).

[21] D. Marcuse, Bell Syst. Tech. J. **51**, 229 (1972).

[22] T. Tamir, *Guided-Wave Optoelectronics* (Springer, New York, 1988).

[23] K. Kawano and T. Kitoh, *Introduction to Optical Waveguide Analysis: Solving Maxwell's Equation and the Schrödinger Equation* (John Wiley and Sons, New York, 2001).

[24] R. Rokitski, P.-C. Sun, and Y. Fainman, Opt. Lett. **26**, 1125 (2001).

[25] F. Louradour and S. Shaklan, J. Opt. A, Pure Appl. Opt. **1**, L7 (1999).

[26] W. R. White, Michael Dueser, W. A. Reed, and Tsuyoshi Onishi, IEEE Photonics Technol. Lett. **11**, 997 (1999).